Project title: GaSTech

Project ID: 271511

Funding scheme: ERA-Net Cofund ACT (http://www.act-ccs.eu/calls/)

Topic: Research and innovation actions for CO_2 Capture and Storage (CCS)

Starting date of project: 1st of August, 2017

Duration: 36 months

WP N°	Del. N°	Title	Contributors	Lead beneficiary	Nature	Dissemination level	Delivery date from Annex I	Actual delivery date dd/mm/yyyy
3	3.4	Improved gas switching reactor models	Jan Hendrik Cloete (SINTEF), Schalk Cloete (SINTEF)	SINTEF	R	PU	31/01/2019	31/01/2019

1 Summary

Significant improvements have been made on the reactor modelling front in the GaSTech project. To date, work in WP3 and WP4 has relied on a 0D reactor model that allows for rapid assessments of gas switching reactor performance for integration into process simulations. As detailed in this report, the 0D model has seen substantial improvements to better represent the different gas switching reactor concepts and achieve faster connection to the process simulations.

In addition, a detailed reactor model using the filtered Two Fluid Model (fTFM), a computational fluid dynamics (CFD) approach, has been developed. This model will be primarily used to determine the correct reactor size for the economic assessments ongoing in WP4. In this report, the model is demonstrated by investigating the potential to reduce the height of the GSR reactors.

The combination of 0D reactor models (rapid assessment of new process concepts based on gas switching technology) and detailed fTFM reactor models (reactor sizing and design optimization) will ensure successful completion of the primary objective of WP3 and WP4: delivering reliable techno-economic assessments of several promising gas switching process concepts.

2 Model improvements

2.1 0D reactor model

Since the submission of D3.1 (Initial gas switching reactor models), several improvements have been made to the 0D simulation code to make the gas switching simulations faster and to add additional features. These improvements are very briefly described here.

2.1.1 Updated initial state

The code has been modified to use the end conditions of the last simulation (reactor temperature and gas and solids compositions) as the initial conditions to the first cycle of the next simulation. This allows a steady reactor behaviour to be reached by running fewer gas switching cycles, enabling faster linking to the process models.

2.1.2 Delayed outlet switch

It has previously been found that the undesired mixing between steps in the gas switching cycle can be reduced by delaying the switching of the outlet valves compared to the switching of the inlet valves [1]. However, the time of the delay changes with the gas inflow conditions and the reactor volume. It was found that the delay time can be automated by specifying the fraction of reactor gas volume that should be displaced by the incoming gas flow. An optimal value of 0.76 reactor volumes displaced was found to minimize the mixing between the steps.

2.1.3 Oxygen carrier utilization

When considering the assumptions of CSTR behaviour and chemical and thermal equilibrium that are used in the 0D model of the gas switching fluidized beds, for any reactor volume and gas inlet flow rate, the amount of mixing between steps, as well as the temperature variation during steps, will be proportional to fraction of oxygen carrier that is converted during a switching cycle. Therefore, the code was modified to enable specifying the oxygen carrier utilization (instead of the step times in seconds) for the different gas switching technologies.

2.1.4 Different heat management strategies for GSC

In the gas switching combustion (GSC) process, a large amount of surplus air has to be added during the oxidation step to cool the reactor. This increases the temperature variation over a cycle and decreases the average turbine inlet temperature for power generation. Such a lower turbine inlet temperature has been shown to negatively impact the net electrical efficiency of the power plant.

The turbine inlet temperature can be increased (for a specified amount of mixing between the steps, and therefore a specified carbon capture efficiency) by recycling some of the depleted air from the oxidation step outlet to the oxidation step inlet. This causes a gradual temperature increase during the entire oxidation step, resulting in a higher average temperature for the oxidation step. This behaviour is illustrated in Figure 1.

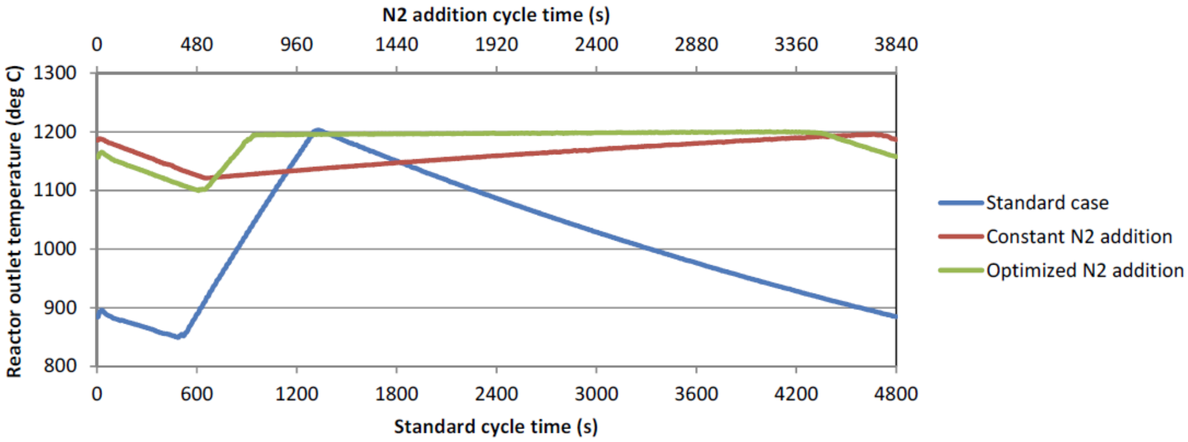

Figure 1 - Temperature variation of the reactor outlet stream for three different operating procedures: the standard case, a case with a constant addition of N_2 in the air stage, and a case with N_2 addition optimized to keep the reactor at its maximum operating temperature for as long as possible. [2]

However, the recycling strategy will require additional process complexity and, in some process configurations, the depleted air stream is required by other parts of the plant. An alternative method is to design the reactor in a way that the air is injected in a very concentrated way. This will allow some of the oxygen to pass through the bed without reacting, limiting the temperature rise during the oxidation step and ideally achieving the same performance as the nitrogen recycle strategy. However, this will add complexity to the reactor design which will have to be investigated with more detailed reactor modelling.

For now, it is assumed that the O_2-slip strategy is feasible and both the nitrogen recycle and O_2 slip strategy has been implemented in the 0D model.

2.1.5 Steam purge in GSC & GSOP

The undesired mixing when switching between steps leads to a decrease in the CO_2 capture efficiency and the CO_2 purity that can be achieved by the process. A possible option for reducing the mixing between the steps is to apply a steam purge between the steps, making essentially zero mixing possible. However, this steam must be generated in the process and using steam therefore leads to a penalty in the efficiency of the power plant. Steam purging has been implemented in the 0D model and an example is shown in Figure 2.

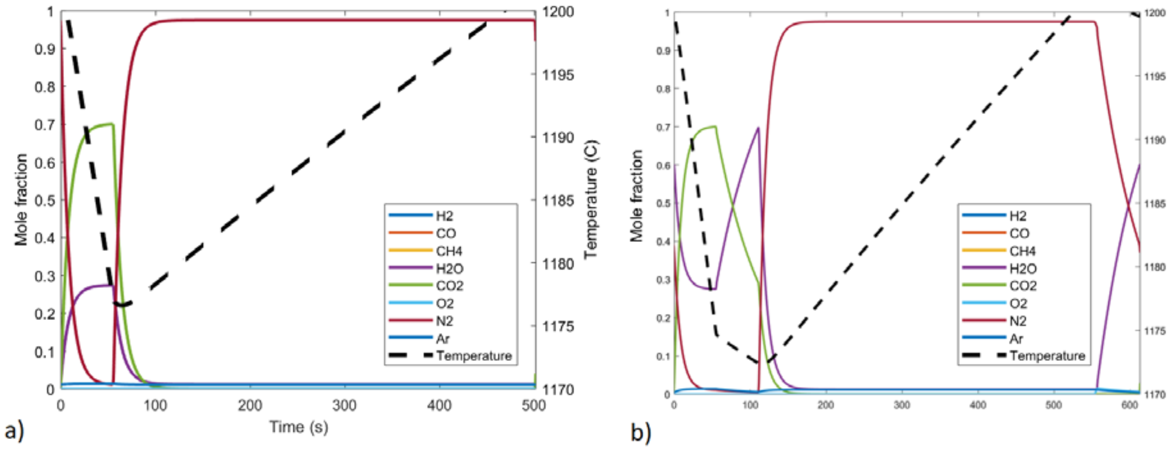

Figure 2 – A cycle of the GSC process a) without and b) with a steam purge between the reduction and oxidation steps. In the case with the steam purge the mixing of CO_2 into the air step and nitrogen into the reduction step is significantly reduced compared to panel a).

2.1.6 Split sweep gas in GSOP

In the gas switching oxygen production (GSOP) process, a sweep gas is added in the reduction step to limit the temperature rise. A potential strategy is to feed the fuel and the sweep gas during reduction in two separate steps. This can produce a stream that contains a higher average oxygen fraction. Since this stream is generally utilized in a gasifier, a higher oxygen content will increase the performance of the gasifier. Such a strategy was therefore implemented in the 0D model, as shown in Figure 3.

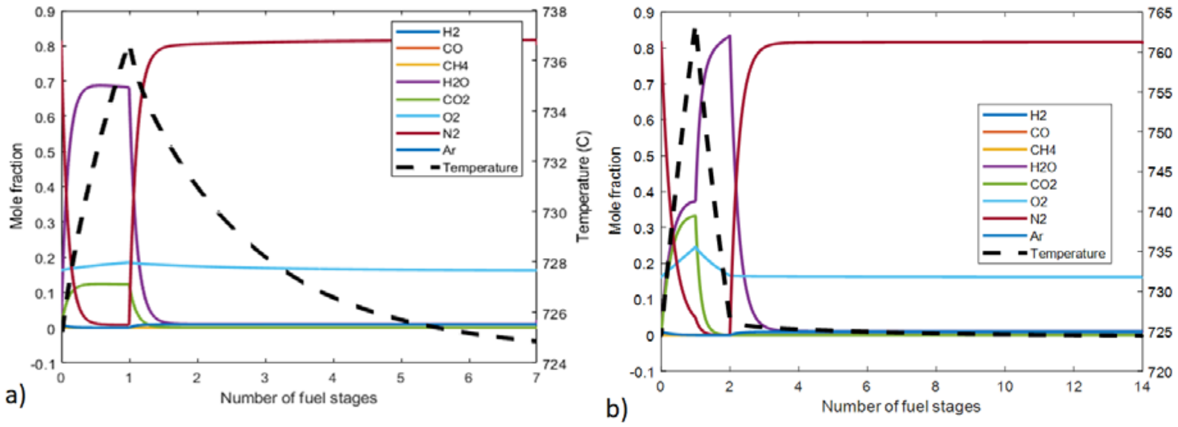

Figure 3 – A cycle of the GSOP process with a) the fuel and the sweep gas mixed in the reduction step and b) the fuel and the sweep gas supplied in separate steps. A higher average oxygen concentration in achieved with the strategy on the right.

2.1.7 Inclusion of syngas treatment in GSR model

In the gas switching reforming (GSR) process, the syngas produced in the reforming step is treated in water gas shift (WGS) and pressure-swing absorption (PSA) units to produce pure hydrogen. The remaining fuel and flue gases in the PSA off-gas is then used in the GSR reduction step. Since the PSA off-gas composition, temperature and flow is determined by the WGS, PSA and heat integration in the process, an iterative procedure between the reactor and process simulations is required. To enable reasonable estimation of reactor behaviour without linking to the process model, simplified modelling of the WGS and PSA units was included in the 0D modelling to estimate the PSA off-gas conditions.

2.2 CFD model

A computational fluid dynamics (CFD) approach will be used in GaSTech to estimate the size of the gas switching fluidized bed reactors, required for economic assessment of the power and hydrogen production processes evaluated in the project. The most common approach for modelling fluidized bed with CFD, is the Two Fluid Model (TFM). In this approach, the particles are approximated as a continuous phase and closures based on the Kinetic Theory of Granular flow [3, 4] are used to account for the translation and collisions of individual particles. However, a drawback of this approach is that a fine computational grid is required to resolve the transient multiphase structures (gas bubbles and particle clusters) that are essential for accurately predicting fluidized bed behaviour. As a result, the TFM is too computationally expensive to give accurate results of the industrial scale fluidized beds considered in GaSTech.

As a solution to this problem, a filtered Two Fluid Model (fTFM) is employed for the CFD modelling, using closures developed previously at SINTEF [5-7]. In the fTFM, simulations are performed on a coarse computational grid, resulting in reasonable computational times for the large reactor geometries considered. Closures, derived from periodic fine-grid TFM simulations, are then used to account for the effects of bubbles and clusters that are not resolved on the coarse grid. These sub-grid structures will influence the drag, particle stresses, reactions and heat transfer. This section will briefly describe the progress made in further developing, testing and implementing the fTFM that will be used in GaSTech.

2.2.1 Evaluation against industrial-scale fluidized bed boiler

This short study investigated the use of an fTFM to model an extremely large (30 m high) industrial fluidized bed boiler. The main findings relevant to GaSTech are summarized here, whereas more details can be found in the published conference paper [8].

- Significant uncertainty exists when extrapolating the closures to grid sizes that are larger than the domains considered in the derivation. Fortunately, preliminary results (see section 3.2) indicate that relatively small reactors will be suitable for GaSTech, limiting the uncertainty at extremely large grid sizes, as required for this case.
- Significant uncertaintly exist when using the fTFM at different particle and fluid conditions than used in the derivation. Although the closures are scaled to account for these changes, it has been found that the accuracy of the scalings is limited [9]. Therefore, where possible, the conditions of the GaSTech reactors will be chosen to minimise this uncertainty.
- Using a filter-to-grid-size ratio of 2 (as is common in literature, e.g. in the work of Ozarkar, Yan [10]) resulted in an unrealistic behaviour when changing the particle size. The scaling of the closures give more realistic results when specifying a filter-to-grid-size ratio of 1 in the closures.

- The anisotropic drag closures recently proposed by our group [6] performs similarly or better than an isotropic drag closure, which is the common approach in literature.

2.2.2 Validation against lab-scale experiments

The anisotropic drag closures for the fTFM developed previously in our group [6] and which will be used in GaSTech, has been validated against experimental data over a range of fluidization velocities and shows good generality. The experimental data [11] consists of average solids volume fractions in a lab-scale fluidized bed with fluidization velocities ranging from 0.06 m/s to 1.4 m/s. Figure 4 gives a qualitative impression of the cases considered, and also shows the deviation of the simulation predictions from the experimental results. The results give confidence for using the developed fTFM in GaSTech.

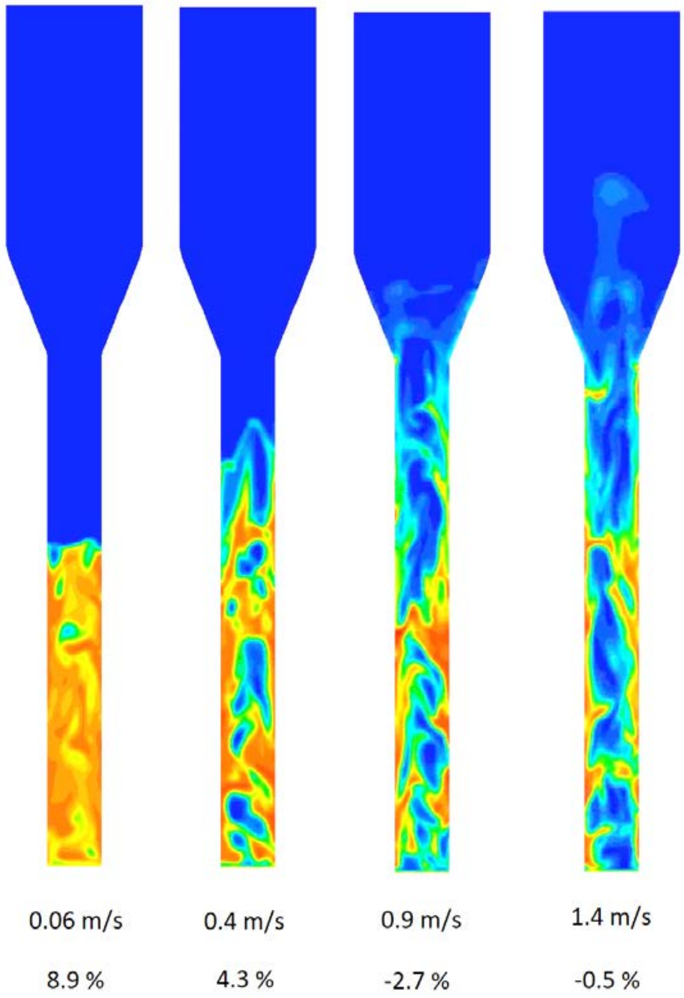

Figure 4 - Instantaneous contour plots of the solids volume fraction (blue = no solids, red = maximum packing) along the centre line for the four validation cases considered. The numbers below each case indicate the fluidization velocity (m/s) and the deviation from the experimental axial bed density (%).

2.2.3 Improved reactive closures

The clusters and bubbles in fluidized beds will also impose a mass transfer limitation to solids catalysed reactions, since the reactant will have to be transported by diffusion into the clusters where it can react. The closures available in literature [12] are limited to first order reactions and are therefore not generally applicable. Therefore, a more general approach has been developed, since more complex reactions will have to be modelled for the gas switching reactors.

Using intra-particle mass transfer theory, a cluster-scale Thiele modulus can be defined as follows:

$$\phi = \sqrt{\frac{n+1}{2}\frac{k_i C_i^{n_i-1}\left(d_p\mathcal{L}\right)^2}{D}} \tag{Equation 1}$$

Here, $\mathcal{L}$ is the ratio of the cluster diameter to the particle diameter, which will be closed in what follows.

For a catalytic reaction, the effectiveness factor can then be written as follows:

$$\eta = \frac{1}{\phi}\left(\frac{1}{\tanh(3\phi)} - \frac{1}{3\phi}\right) \tag{Equation 2}$$

This relation is exact for a first order reaction in a porous particle with no convective transport. Relatively small discrepancies arise for reactions of different order, but the largest uncertainty in this application is the constant deformation of the clusters in the fluidized bed, as well as the convective species transport taking place inside the cluster.

The basic premise of this approach is that the effectiveness factor in Equation 2 represents the largest achievable mass transfer resistance (smallest effectiveness factor). This will typically occur at intermediate filtered solids volume fractions when maximum phase segregation is achieved and clusters are relatively large. As the filtered solids volume fraction tends to the limits of zero or maximum packing, clustering disappears and the mass transfer resistance tends to zero ($\eta = 1$).

A hypothesis can then be formulated that, for different Thiele moduli, the minimum effectiveness factor (η_{min}) can be scaled by using Equation 2, while the tendency towards $\eta = 1$ will be proportional to η_{min}. In other words, when a filtered effectiveness factor model (η_{ref}) is derived for a reference Thiele modulus (ϕ_{ref}), a new effectiveness factor (η_{ref}) can be estimated for another Thiele modulus (ϕ_{new}) as follows:

$$\eta_{new,min} = \eta_{ref,min}\frac{\frac{1}{\phi_{new}}\left(\frac{1}{\tanh(3\phi_{new})} - \frac{1}{3\phi_{new}}\right)}{\frac{1}{\phi_{ref}}\left(\frac{1}{\tanh(3\phi_{ref})} - \frac{1}{3\phi_{ref}}\right)} \tag{Equation 3}$$

$$\eta_{new} = 1 - (1 - \eta_{ref})\frac{(1 - \eta_{new,min})}{(1 - \eta_{ref,min})} \tag{Equation 4}$$

This scaling of a filtered effectiveness factor model from ϕ_{ref} to ϕ_{new} should hold as long as the change in the reaction rate does not make a large change to the cluster dynamics.

The reference effectiveness factor, η_{ref}, is calculated using a simple 1-marker closure, with the filter size and solids volume fraction as independent variables, based on a previously derived closure in our group [13]. The cluster length scale, $\mathcal{L}$, was found to increase with the filter size (proportional to the grid size used in the coarse grid simulations) and can be calculated as:

$$\mathcal{L} = 15.5\left(\frac{2}{\pi}\right)\operatorname{atan}\left(0.669\Delta_f^*\right) \qquad \text{Equation 5}$$

Here, Δ_f^* is the dimensionless filter size. From the closure of $\mathcal{L}$, the cluster size will tend toward 15.5 times the particle size at very large grid sizes.

Figure 5 shows an example of the performance of the approach outlined above. In a second order solids catalysed reaction the effectiveness factor will increase with increasing conversion of the reactant. Figure 5 shows that the proposed approach performs very well.

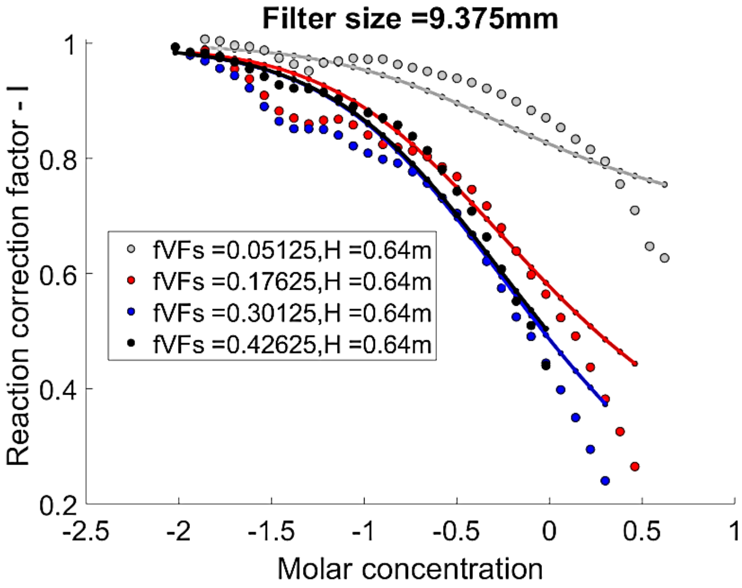

Figure 5 – The effectiveness factor of a second order solids catalysed reaction as a function of the molar concentrations (mol/m^3) of the gas-phase reactant. The dots show the results from fine-grid fTFM simulations, while the lines show the model predictions. The different colours show different solids volume fractions.

Additionally, Figure 6 shows the performance of the reactive fTFM approach when verifying the coarse-grid simulations against fine-grid TFM simulations in a turbulent fluidized bed. The proposed approach performs well for a range of reaction rates and reaction orders and is therefore deemed suitable for further use in the GaSTech project.

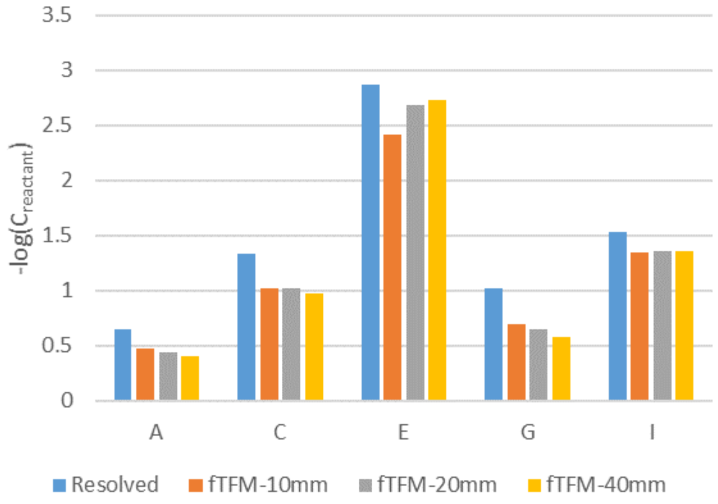

Figure 6 – Resolved (fine-grid) TFM simulation results compared to coarse-grid fTFM results for different reactions. Case C is the reference first-order reaction for which the closures were originally derived. In Case A, the reaction rate is decreased by a factor of 4 and in Case E it is increased by a factor of 4. Case G and Case I are for reaction orders of 0.5 and 2, respectively, where the reaction rate constant is the same as in Case C.

3 Reactor simulations

3.1 0D model

The improved 0D model has already been used in several process studies based on gas switching technologies. A brief summary is given in this section.

3.1.1 GSC

The use of the 0D model for GSC was already shown in section 2.1.5 and will therefore not be repeated here. GSC reactor simulations were performed as part of a recently accepted journal paper [14]. This process modelling study (performed by UPM) found that a GSC-IGCC power plant can even exceed the efficiency of an unabated IGCC plant, when used in combination with an additional combustor after the GSC reactors and improved heat integration. Ultimately, the most efficient plant evaluated in this study achieved 50.9% efficiency with 80.7% CO_2 capture.

3.1.2 GSOP

The GSOP technology was recently studied as part of a novel oxygen production pre-combustion (OPPC) IGCC power plant [15]. The OPPC-IGCC plant integrates a GSOP unit into a pre-combustion IGCC power plant, reducing the energy penalty through two channels: 1) avoidance of a cryogenic air separation unit and 2) pre-heating the air sent to the combined power cycle, which reduces the steam requirement for shifting CO to H_2 and the CO_2 capture duty involved in pre-combustion CO_2 capture.

To describe the reactor behaviour for the GSOP process, Figure 7 shows the reactor outlet temperature and compositions over a full reactor cycle for six different cases. In all cases, it can be seen that, during the fuel stage, the fuel is combusted to H_2O and CO_2 by oxygen from the oxygen carrier, also releasing heat which increases the outlet temperature. Additionally, the oxygen carrier releases oxygen which can be used in the gasifier. In the subsequent oxidation stage, the oxygen carrier is regenerated by air.

Despite this reaction being exothermic (ΔH = -91 kJ/mol), the reactor temperature decreases due to the large amount of air that must be heated up and the relatively small fraction of the oxygen in air that reacts with the oxygen carrier.

At the start of the oxidation stage, the undesired mixing of CO_2 into the oxidation stage products, which will reduce the carbon capture efficiency, can be observed. Furthermore, it can be seen that the oxygen mole fraction in the reactor outlet follows the trends of the reactor temperature due to the equilibrium reaction between the oxygen carrier and oxygen. Due to the non-linear trend of the temperature in the oxidation stage, the average oxygen mole fraction in the oxidation stage will tend to be lower than that in the reduction stage. This difference will be greater for cases with relatively more air being added (longer dimensionless cycle time when scaled by the fuel stage time) since the temperature profile flattens out more during the longer air stages.

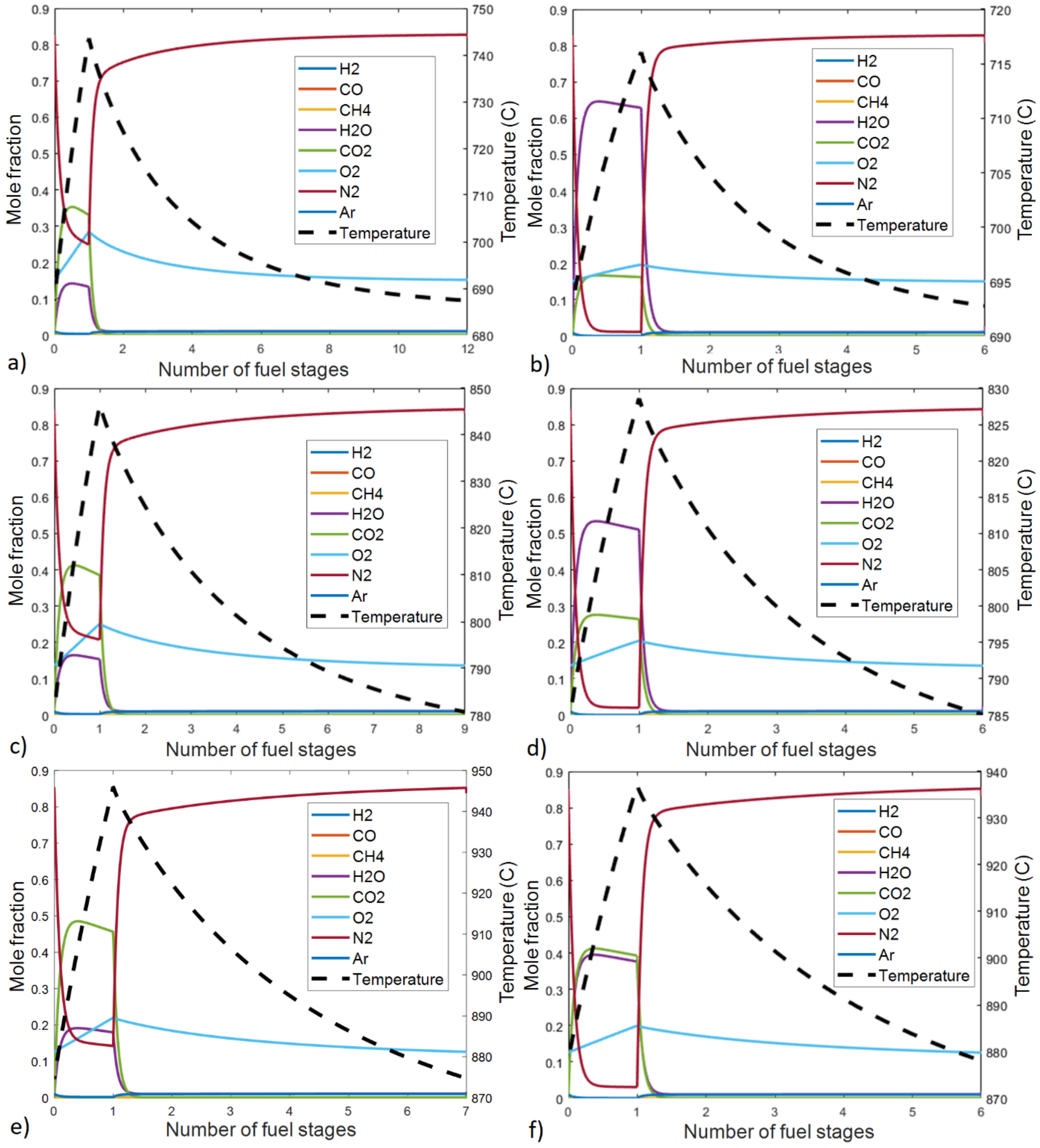

Figure 7: Temperature and compositions at the reactor outlet during a full cycle for different reactor simulations. The left column shows Air to Gasifier cases and the right column Steam to GSOP cases. From top to bottom the rows show cases with average oxidation stage temperatures of 700°C, 800°C and 900°C.

In this study, two ways were explored to supply enough O_2 to the gasifier: 1) feeding additional steam to the GSOP reduction stage inlet to increase the amount of sweep gas and enable more extraction of free O_2 from the oxygen carrier (henceforward Steam to GSOP cases) and 2) adding air to the GSOP reduction stage outlet to directly increase the oxygen flowrate in the stream to the gasifier (henceforward Air to Gasifier cases).

The primary difference between the Air to the Gasifier cases (left-hand column in Figure 7) and the Steam to GSOP cases (right-hand column in Figure 7) is the composition of the reduction stage outlet stream, which is diluted by nitrogen in the Air to Gasifier cases and by steam in the Steam to GSOP cases. For the Air to Gasifier cases, the length of the oxidation stage decreases substantially with increasing reactor temperature. This is because, at higher reactor temperatures, the incoming air stream must be heated to a higher temperature and therefore less air is required to remove the combustion heat from the reactor.

The process modelling (UPM) found that, relative to a conventional pre-combustion IGCC benchmark, the OPPC configuration improves the electric efficiency by about 6 %-points, although the CO_2 capture ratio reduces by about 6 %-points. Plant efficiency also benefits from an increase in GSOP operating temperature, although the maximum temperature was limited to 900 °C to avoid any temperature-related challenges with oxygen carrier stability or downstream valves and filters. OPPC therefore appears to be a promising configuration for minimizing the energy penalty of CO_2 capture in IGCC power plants.

3.1.3 GSR

The 0D model has recently been utilized in two GSR process studies. In the first [16], improved heat integration was undertaken to improve the efficiency of a GSR-combined cycle power plant.

It was found that the temperatures during the oxidation, reduction and reforming steps of the GSR are higher in the cases of heat integration. This is because the heat recovered from the syngas and CO_2 stream from the GSR is recirculated back to the GSR through pre-heating of inlet streams during the reduction and reforming steps. As seen in Figure 6, the higher inlet temperatures lead to a smaller drop in the reactor temperature during the reduction (0-300 s) and reforming (300-900 s) stages compared to the cases without heat integration. This, in turn, results in higher average temperatures during each of the stages, considering that the maximum temperature in the cycle is always fixed to 1100 °C.

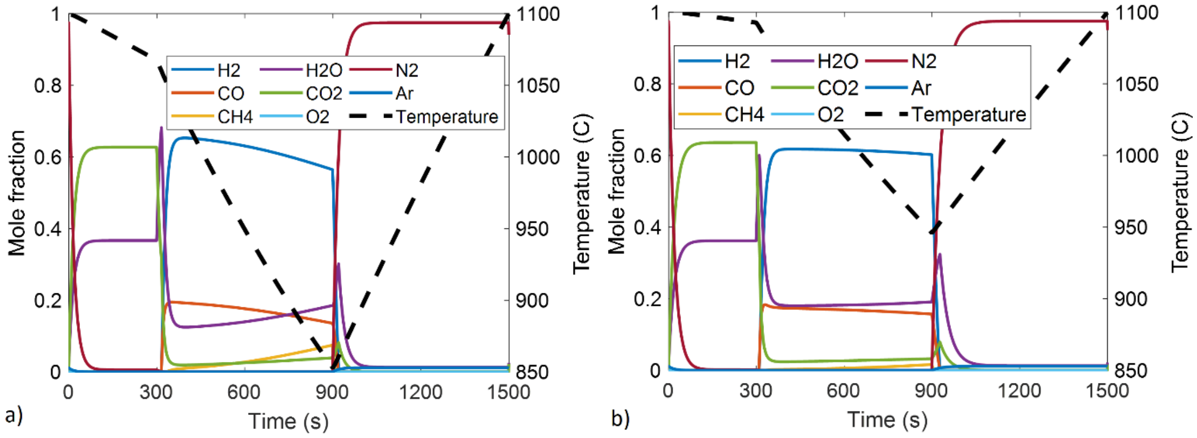

Figure 8: The composition and temperature at the reactor outlet during a cycle for a) the cases with improved GSR-CC without heat integration and b) the cases with improved GSR-CC and heat integration.

From the process modelling (performed by NTNU), a net electrical efficiency of 51.1 % was obtained. The efficiency penalty in the improved GSR-CC process is only 7.2 %-points with respect to the reference case natural gas combined cycle power plant without CO_2 capture, and is less than post-combustion capture methods presented in literature. The CO_2 avoidance in the GSR-CC is more than 95%. GSR-CC also gives a flexibility in the output from the plant in terms of pure H_2 or electricity and the optimal plant configuration is designed to maximize this flexibility.

In the second study [17], a GSR process for hydrogen production with integrated CO_2 capture at a minimal energy penalty was investigated. Among other things, the effect of GSR reactor pressure was studied with the 0D model, as shown in Figure 4. The oxygen carrier utilization is kept proportional to the pressure to keep the mixing between the steps similar for different cases. Consequently, the step length increases with increasing reactor pressure. As a result, the temperature variation across the cycle is larger in Figure 4.a than in Figure 4.b. Since the maximum temperature in the cycle is maintained at 1100 °C, this leads to lower temperatures being reached in the higher pressure cases, which results in a lower average methane conversion across the entire reforming step. This is clearly visible in Figure 4, where the 32.7 bar case showed significant CH_4 slip towards the end of the reforming step, while CH_4 conversion in the 15 bar case is almost complete.

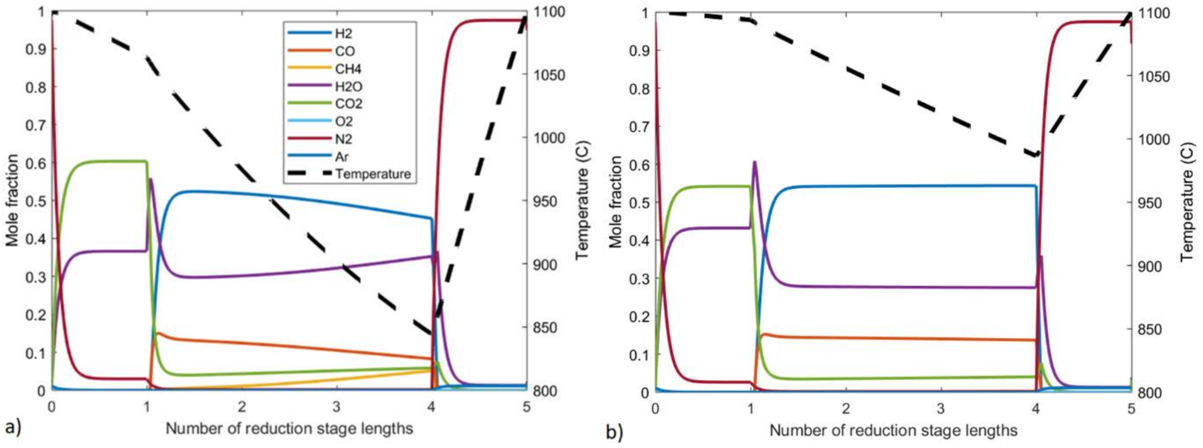

Figure 9: The temperature and composition as a function of the number of reduction step lengths for a full cycle of the GSR for a) a reactor pressure of 32.7 bar and b) a reactor pressure of 15 bar. The reduction step lengths are 401 s and 136 s respectively.

The process simulations (NTNU) found that, at the optimal operating pressure (and in combination with additional thermal mass in the reactor, as discussed in the next section), the GSR-H2 plant could eliminate the energy penalty of CO_2 capture for hydrogen production.

3.2 CFD model

The 0D model used thus far the GaSTech WP3 activities assumes complete reactant conversion to the thermodynamic limits of the process. It does not give any information on the size of the reactor that will be required to achieve this pre-set condition. More detailed reactor modelling using computational fluid dynamics (CFD) is required to address this shortcoming and allow for reasonable reactor sizing in the economic assessments ongoing in WP4. A filtered Two Fluid Model (fTFM) has been developed for this purpose and applied to the GSR concept as detailed below.

3.2.1 fTFM simulation of the GSR reactor

The GSR simulations thus far completed in GaSTech assume the use of a highly active NiO oxygen carrier. This highly reactive oxygen carrier offers the potential for intensifying the GSR process into relatively small reactors that can substantially reduce the capital costs and fixed operating costs of plants based around the GSR concept.

The fTFM was used to simulate such a reactor. Due to the computational expense of this much more detailed modelling approach, only the part of the GSR cycle that exhibits the slowest reaction rates will be simulated as an example in this report. This part occurs at the end of the reforming stage when the reactor temperature reaches a minimum (see Figure 4). Since the reaction rates increase exponentially with temperature, this lowest temperature point will be where the complete conversion assumption in the 0D model is the most uncertain.

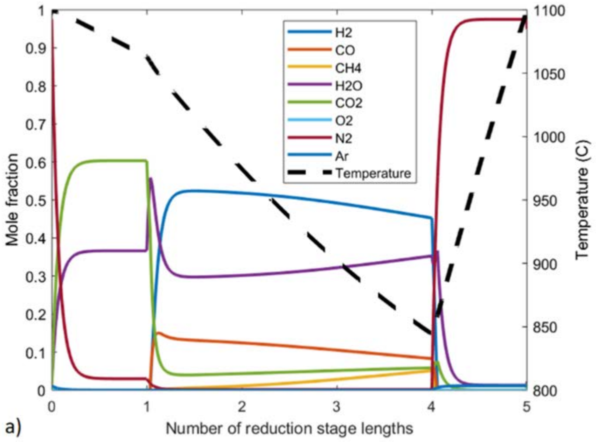

Figure 10: The temperature and composition as a function of the number of reduction step lengths for a full cycle of the GSR (simulated using the 0D model). The fTFM simulation in this report is carried out at the lowest temperature that occurs at the end of the reforming stage (number of reduction stage lengths = 4).

A 3D model of a simple cylindrical GSR reactor carrying out reforming at a temperature of 1100 K (lowest cycle temperature at the end of the reforming stage) was constructed and run. The reactor diameter was set to 1.23 m, which will result in a cross-sectional area where a cluster of 10 such GSR reactors can process 10 ton/h of natural gas feed at 32.7 bar pressure with a superficial gas velocity of 0.4 m/s. The height of this reactor required to get sufficiently close to the equilibrium conversion assumed in the 0D model is the main variable that should be determined by the detailed reactor model.

To investigate this topic, three reactor simulations were completed at three different aspect ratios: 3, 1.5 and 1. It can be noted here that a recently completed economic assessment in the GaSTech project showed that an efficient integration of the GSR concept for H_2 production could capture 95% of CO_2 at a cost that is 3% lower than the benchmark steam-methane reforming process with no CO_2 capture. In other words, GSR can achieve profitable hydrogen production with CO_2 capture even without any CO_2 tax. This result was achieved by assuming an aspect ratio of 3, so further reductions in the reactor length will further improve the competitiveness of the GSR H_2 production process.

Figure 5 and Figure 6 show some qualitative results from these three simulations. It is immediately clear from Figure 6 that equilibrium is achieved quite low down in the tallest reactor, implying that the

0D assumption of complete conversion will be valid for this reactor height. For the other two cases, equilibrium conversion is not completely achieved.

Figure 5 also shows that the taller bed is denser in the lower regions, which results in an even faster reaction rate in this zone where the species concentrations are far from equilibrium and the reaction rate is high. For this reason, the reactant conversion at the bottom of the bed is faster in the aspect ratio 3 case than for the other two cases, as shown in Figure 6.

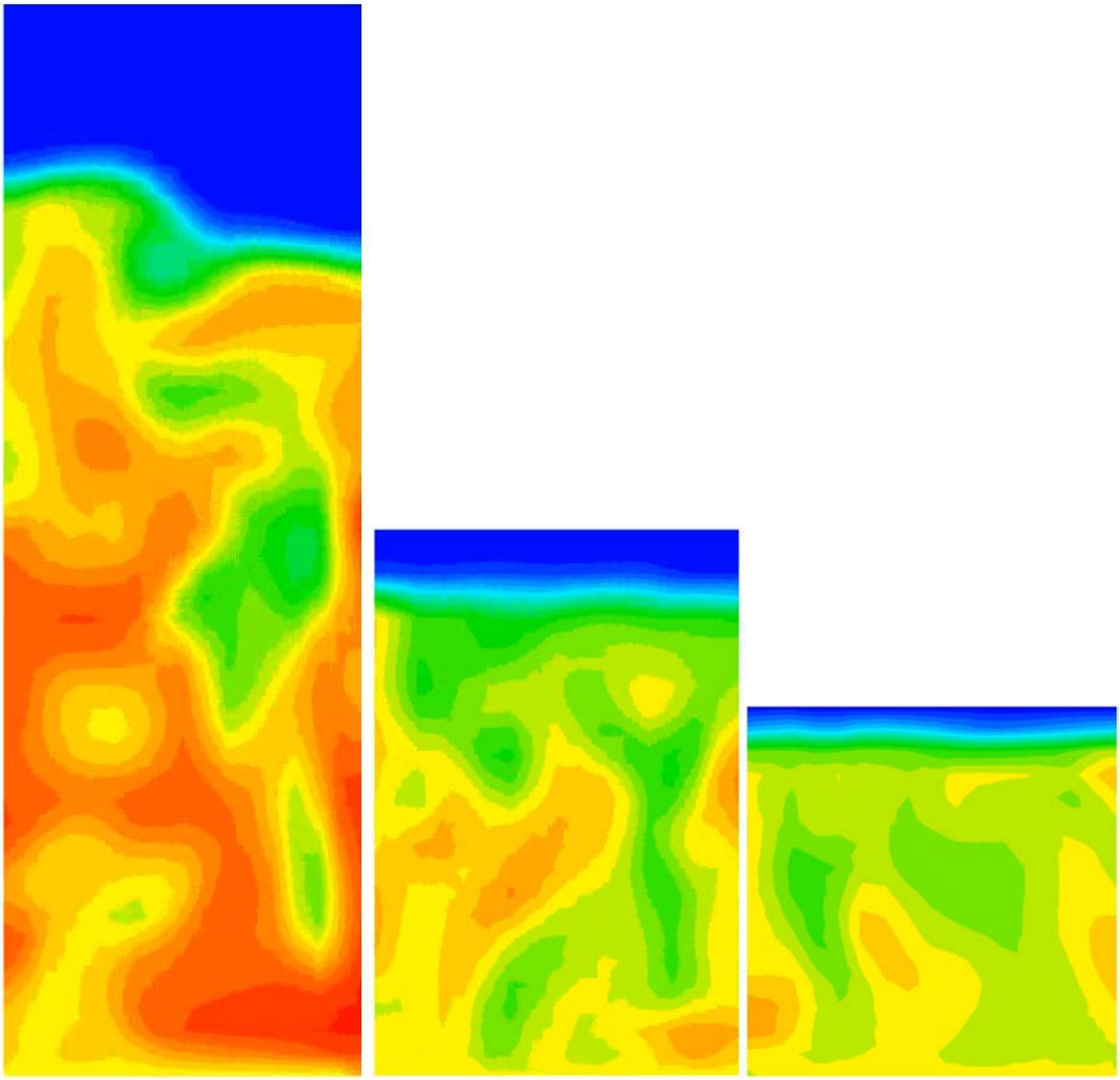

Figure 11: Instantaneous contour plots of volume fraction for the three reactor simulations at aspect ratios of 3, 1.5 and 1. The blue-green-red colourmap ranges from 0 (blue) through 0.3 (green) to 0.6 (red).

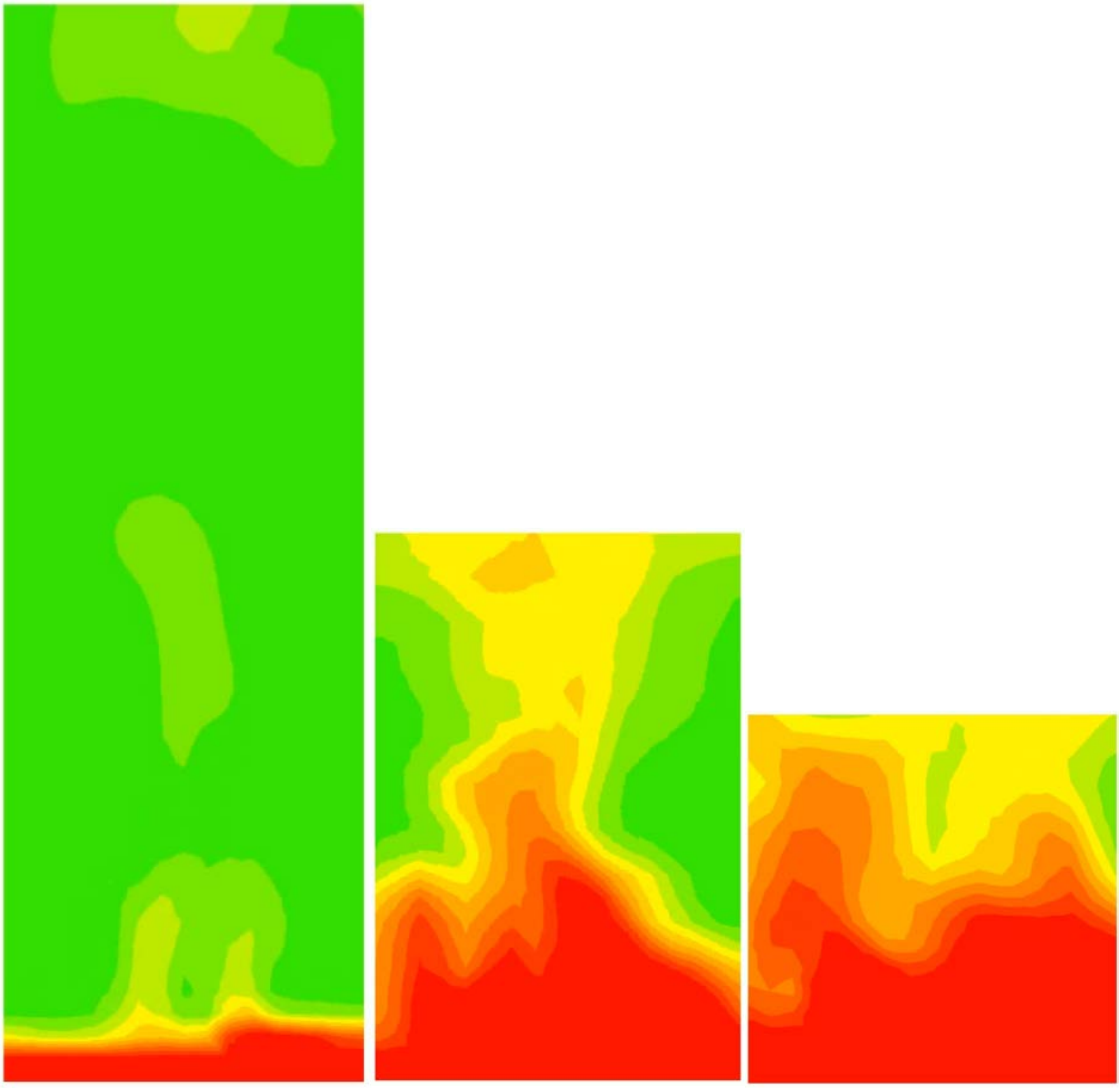

Figure 12: Instantaneous contour plots of CH_4 mol fraction for the three reactor simulations at aspect ratios of 3, 1.5 and 1. The blue-green-red colourmap ranges from 0 (blue) through 0.05 (green) to 0.1 (red).

It should be noted that slightly less than equilibrium conversion at this slowest point in the GSR cycle will have a minimal effect on the overall degree of CH_4 conversion achieved. The remaining part of the reduction cycle takes place at higher temperatures, leading to faster reaction rates. Thus, if equilibrium conversion is almost achieved at the lowest temperature point, complete conversion will take place for most of the reforming stage, minimizing the overall reduction in CH_4 conversion from the whole cycle. More computationally expensive fTFM simulations carried out over the entire GSR cycle will investigate this effect in more detail in the near future.

Quantification of the conversion performance in the three simulations is shown in Figure 7 where the observations from Figure 6 are confirmed: The aspect ratio of 3 achieves complete equilibrium conversion (almost no change in the species mol fractions takes place in the upper reactor regions), whereas equilibrium is almost achieved in the shorter reactors.

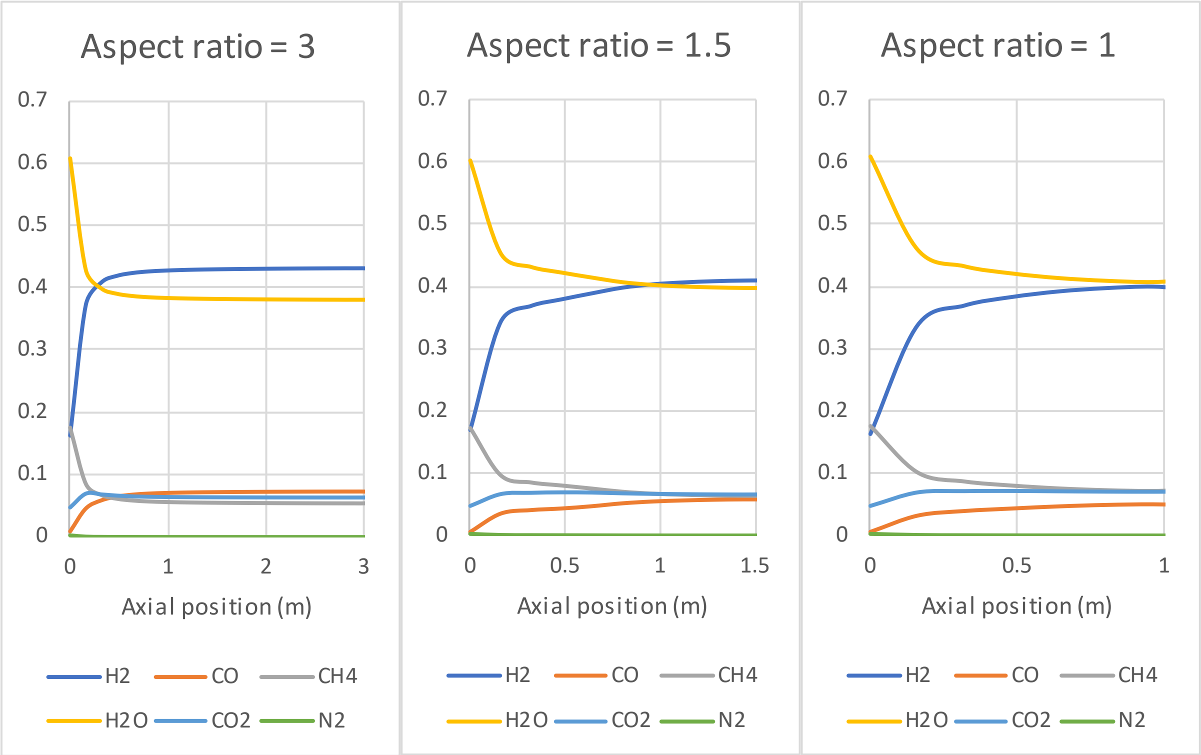

Figure 13: Axial species mol fraction profiles averaged over 30 s of simulation time and across the reactor cross-sectional area for the three cases with aspect ratios of 3, 1.5 and 1.

Future work will use this model to investigate whether a smaller reactor that does not quite achieve equilibrium conversion can improve process economics. Given that the reactors are already quite small (and reasonably cheap), further reductions in reactor costs are unlikely to have a large influence on the cost of H_2. It is therefore likely that that optimum point lies close to the point achieving full conversion, possibly an aspect ratio around 2 in this case.

The fTFM will also be employed to investigate reactor designs with added thermal mass in the form of metal rods inserted into the reactor. As shown in Figure 8, the addition of thermal mass (doubling of the heat capacity in the reactor) halves the temperature drop in the reforming stage. This not only enhances the equilibrium conversion of CH_4, but also achieves higher reaction rates, potentially allowing for even smaller reactors.

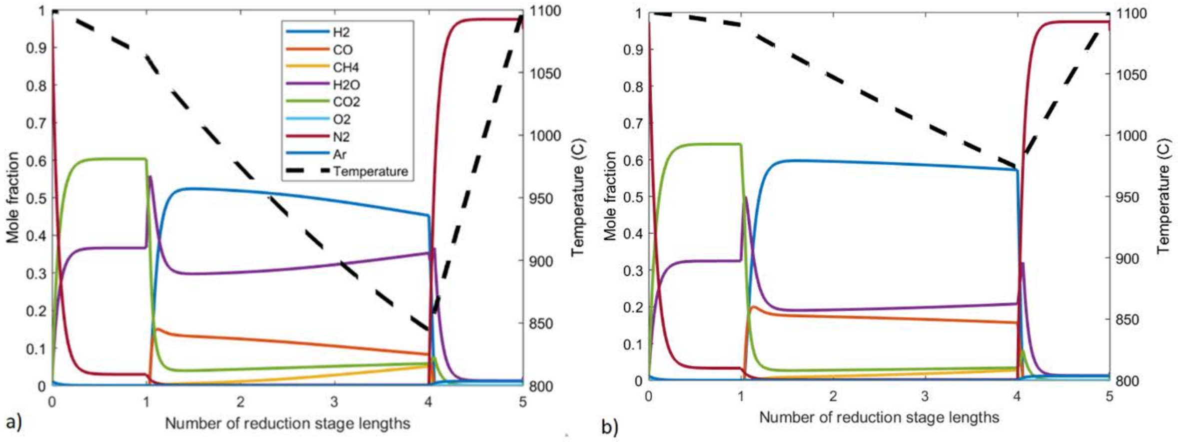

Figure 14: The temperature and composition as a function of the number of reduction step lengths for a full cycle of the GSR for a) without and b) with added reactor thermal mass.

The addition of metal rods will influence the reactor hydrodynamics, making the detailed fTFM more important for reactor design and optimization of the trade-off between reactor size and conversion. In addition, the dimensions, positioning and overall volume fraction of metal rods inserted into the reactor will play an important role in minimizing the reactor cost, while maximizing reactor performance to minimize the ultimate cost of hydrogen. All these aspects will be investigated in future work with the detailed reactor model presented in this report.

4 Conclusion

Since the submission of D3.1, the 0D reactor model has been improved by adding several features to enable the simulation of different gas switching technologies. The code has successfully been utilised in studying several process configurations and has contributed to several journal papers. On the other hand, a more detailed simulation approach using CFD and the fTFM has been developed, verified, validated and applied to the GSR process.

In the remainder of the project, the 0D model will continue to be used for fast coupling with the process modelling to investigate other promising hydrogen and electricity production concepts with CO_2 capture. The CFD reactor model will be used to study more detailed reactor design issues and to provide estimate reactor sizes for economic assessments.

5 References

1. Cloete, S., et al., *Integration of a Gas Switching Combustion (GSC) system in integrated gasification combined cycles.* International Journal of Greenhouse Gas Control, 2015. **42**: p. 340-356.
2. Cloete, S., et al., *Heat management in Gas Switching Combustion for power production with integrated CO2 capture*, in *7th International Conference on Applied Energy* 2015.
3. Lun, C.K.K., et al., *Kinetic Theories for Granular Flow: Inelastic Particles in Couette Flow and Slightly Inelastic Particles in a General Flow Field.* Journal of Fluid Mechanics, 1984. **140**: p. 223-256.
4. Gidaspow, D., R. Bezburuah, and J. Ding, *Hydrodynamics of Circulating Fluidized Beds, Kinetic Theory Approach*, in *7th Engineering Foundation Conference on Fluidization* 1992. p. 75-82.
5. Cloete, S., J.H. Cloete, and S. Amini, *Hydrodynamic validation study of filtered Two Fluid Models.* Chemical Engineering Science, 2018. **182**: p. 93-107.
6. Cloete, J.H., et al., *Development and verification of anisotropic drag closures for filtered Two Fluid Models.* Chemical Engineering Science, 2018. **192**: p. 930-954.
7. Cloete, J.H., et al., *Development and verification of anisotropic solids stress closures for filtered Two Fluid Models.* Chemical Engineering Science, 2018. **192**: p. 906-929.
8. Cloete, J.H., et al., *Evaluation of Filtered Two Fluid Models Against Data from an Industrial Scale Fluidized Bed Reactor*, in *2018 AIChE Annual Meeting*. 2018: Pitssburgh, Pennsylvania.
9. Schneiderbauer, S. and S. Pirker, *The impact of different fine grid simulations on the sub-grid modification for gas–solid drag*, in *9th International Conference on Multiphase Flow*. 2016: Firenze.
10. Ozarkar, S.S., et al., *Validation of filtered two-fluid models for gas–particle flows against experimental data from bubbling fluidized bed.* Powder Technology, 2015. **284**: p. 159-169.

11. Zhu, H., et al., *Detailed measurements of flow structure inside a dense gas–solids fluidized bed.* Powder Technology, 2008. **180**(3): p. 339-349.
12. Holloway, W. and S. Sundaresan, *Filtered models for reacting gas–particle flows.* Chemical Engineering Science, 2012. **82**(0): p. 132-143.
13. Cloete, J.H., *Development of Anisotropic Filtered Two Fluid Model Closures*, in *Department of Energy and Process Technology*. 2018, Norwegian University of Science and Technology: Trondheim, Norway.
14. del Pozo, C.A., et al., *The potential of gas switching combustion to eliminate the energy penalty of CO2 capture.* International Journal of Greenhouse Gas Control, 2018. **Accepted**.
15. del Pozo, C.A., et al., *The Oxygen Production Pre-Combustion (OPPC) IGCC plant for efficient power production with CO2 capture.* International Journal of Greenhouse Gas Control, 2019. **Under Review**.
16. Nazir, S.M., et al., *Gas switching reforming (GSR) for power generation with CO2 capture: Process efficiency improvement studies.* Energy, 2019. **167**: p. 757-765.
17. Nazir, S.M., et al., *Efficient hydrogen production with CO2 capture using gas switching reforming.* Energy, 2019. **Under review**.